electronics

MDPI

Article

A Compact 3.3–3.5 GHz Filter Based on Modified Composite Right-/Left-Handed Resonator Units

Shanwen Hu [1,*], Yunqing Hu [1], Haiyu Zheng [1], Weiguang Zhu [1], Yiting Gao [1] and Xiaodong Zhang [2]

[1] College of Electronic and Optical Engineering & College of Microelectronics, Nanjing University of Posts and Telecommunications, Nanjing 210023, China; 1217022808@njupt.edu.cn (Y.H.); 1218023006@njupt.edu.cn (H.Z.); 1218023007@njupt.edu.cn (W.Z.); B17020603@njupt.edu.cn (Y.G.)

[2] School of Electronic & Information Engineering, Suzhou University of Science and Technology, Suzhou 215009, China; zhangxd_usts@126.com

* Correspondence: shanwenh@njupt.edu.cn; Tel.: +86-025-85866131

Received: 26 November 2019; Accepted: 17 December 2019; Published: 18 December 2019

Abstract: In the RF (Radio Frequency) front-end of a communication system, bandpass filters (BPFs) are used to send passband signals and reject stopband signals. Substrate-integrated waveguides (SIW) are widely used in RF filter designs due to their low loss and low cost and the flexibility of their integration properties. However, SIW filters under 6 GHz are still too large to meet the requirement of portable communication devices due to their long wavelength. In this paper, a very compact fully integrated SIW filter is proposed and designed with RT6010 dielectric material to meet the small size requirement of portable devices for next-generation sub-6 G applications. The proposed filter contains two sawtooth-shaped composite right-/left-handed (CRLH) resonator units, instead of traditional rectangular-shaped CRLH resonator units, which makes the filter more compact and cost effective. The filter is designed and fabricated on an RT6010 substrate, with a size of only 10 mm × 7.4 mm. The measurement results illustrated that the proposed BPF shows a passband covering the frequency range of 3.25–3.45 GHz; the minimum passband insertion loss is only 2.4 dB; the stopband rejection is better than −20 dB throughout the frequencies below 3.0 GHz and above 3.8 GHz; S11 is as low as −37 dB at 3.35 GHz; and the group delay variation is only 1.4 ns throughout the operation bandwidth.

Keywords: RF filter; SIW; CRLH; compact filter; low-loss filter

1. Introduction

Most commercial communication standards are focused on a frequency band lower than 6 GHz, such as LTE (Long Term Evolution), 5G, Wi-Fi, Bluetooth, Zigbee, etc. In the front-end of a sub-6G communication system, filters play the key role of sending passband signals and rejecting stopband signals. Due to the need to meet the small size requirement of sub-6G portable devices, compact sub-6G filter design has become a hot research topic in recent years. Substrate integrated waveguides (SIWs) are widely used in RF (Radio Frequency) passive device designs due to their low loss and low cost and the flexibility of their integration properties, such as their filter [1–6], antenna [7–9], phase shifter [10–14], power divider [15–18], coupler [19–22], etc. However, SIW filters under 6 GHz are still too large to meet the requirement of portable communication devices because of their long wavelength.

Numerous studies have been presented to reduce the size of SIW filters. Due to the advantage of the zero-order resonance characteristic, which makes the resonance frequency of SIWs relatively irrelevant with respect to the device size [23], a composite right-/left-handed (CRLH) structure is traditionally used to minimize the size of SIW passive devices [24–28]. A rectangular interdigital structure is usually utilized to realize the capacitor and inductor of the resonator for traditional CRLH

filters. However, the size of this rectangular CRLH structure is still too large for sub-6G filters due to its limited coupling capacitance value. A typical rectangular CRLH filter is reported in [25], to have a compact size, and the operation frequency is 6.8 GHz, with an insertion loss of 3 dB, which is beyond the frequency limitation of 6 GHz. In this work, a novel sawtooth CRLH resonator unit is proposed to further realize a compact filter working inside the 6 GHz frequency range. The coupling capacitor of the filter is increased by about 50% with the proposed sawtooth CRLH unit; the transmission loss is reduced to 2.4 dB by the substrate-integrated waveguide; and the working frequency is finally reduced to 3.35 GHz, with a 200 MHz bandwidth. The structure, design theory, and mechanism, simulations, and experimental demonstration of the proposed filter will be discussed in detail in the following sections.

2. Filter Structure and Analysis

An SIW filter based on a conventional CRLH structure [25] is shown in Figure 1a. Two CRLH resonators, composed of interdigital rectangular-shaped metal slots, are coupled with an SIW transmission line (SIW TL). Metallization through holes are placed as vias to connect CRLH units to the backside ground. The SIW TL is adopted to restrict the propagating waves by arrays of vias, which results in the filter having a low loss. The CRLH cells can provide resonators that are independent of their physical lengths, and they can therefore be more compact, especially at lower frequencies [25].

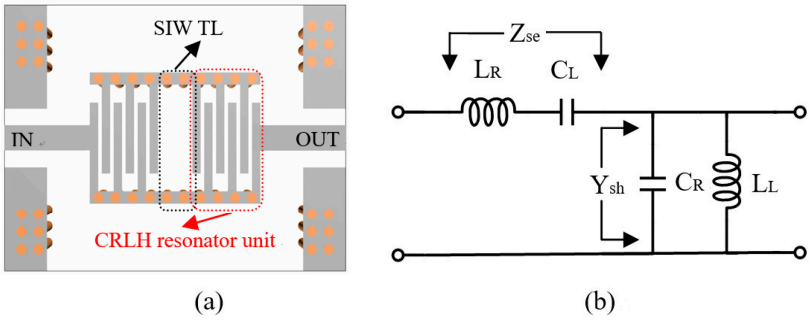

Figure 1. (**a**) Conventional substrate integrated waveguide (SIW) filter with interdigital rectangular composite right-/left-handed (CRLH) units and (**b**) the equivalent circuit of a CRLH resonator unit.

The equivalent circuit of the single CRLH resonator unit is shown in Figure 1b. The filter circuit is composed of a left-hand series capacitor C_L, shunt inductor L_L, right-hand shunt capacitor C_R, and series inductor L_R. Parasitic resistances are usually ignored when analyzing the operation frequency of CRLH filters, since they show little effect on the frequency response. Their contributions are mainly reflected in the introduction of frequency-independent insertion loss. The capacitors of the CRLH units are realized by the interdigital fingers in the structure, and the inductors are generated by the rectangular slots and vias in the structure. The "left-hand" property is performed under a certain frequency range when an electromagnetic wave passes through the structure, and the effective dielectric constant and effective permeability is negative. On the other hand, the "right hand" property is performed under another frequency range, and the effective dielectric constant and effective permeability is positive. Consequently, a complex resonance behavior of this structure can be accomplished to improve the performance of the RF passive devices.

According to the equivalent circuit, shown in Figure 1b, the unit series impedance Z_{se} and shunt admittance Y_{sh} can be written as the following equation:

$$Z_{se} = j\omega L_R + \frac{1}{j\omega C_L} \qquad Y_{sh} = j\omega C_R + \frac{1}{j\omega L_L}. \tag{1}$$

According to the transmission line theory, the transmission constant can be derived as:

$$\gamma = \alpha + j\beta = \sqrt{Z_{se}Y_{sh}}. \tag{2}$$

Assuming the structure is lossless, then $\alpha = 0$. Equation (1) can be applied to Equation (2), and then the phase constant $\beta(\omega)$ can be calculated, as in Equation (3):

$$\beta(\omega) = S(\omega)\sqrt{\omega^2\omega_R + \frac{1}{\omega^2\omega_L} - \left(\frac{L_R}{L_L} + \frac{C_R}{C_L}\right)}. \tag{3}$$

In Equation (3), $S(\omega)$ is a frequency-related parameter under two possible conditions, and if $\omega > \max(\omega_{se}, \omega_{sh})$, then:

$$s(\omega) = \frac{+\omega}{\omega_R}\sqrt{\left[1 - \left(\frac{\omega_{sh}}{\omega}\right)^2\right]\left[1 - \left(\frac{\omega_{se}}{\omega}\right)^2\right]}, \tag{4}$$

if $\omega < \min(\omega_{se}, \omega_{sh})$, then:

$$s(\omega) = \frac{-\omega}{\omega_R}\sqrt{\left[\left(\frac{\omega_{sh}}{\omega}\right)^2 - 1\right]\left[\left(\frac{\omega_{se}}{\omega}\right)^2 - 1\right]}. \tag{5}$$

In the above equation, ω_R indicates the right-hand cutoff frequency, ω_L indicates the left-hand cutoff resonant frequency, ω_{se} represents the series resonant frequency, and ω_{sh} represents the shunt resonant frequency.

$$\begin{array}{ll} \omega_R = \frac{1}{\sqrt{L_R C_R}} & \omega_L = \frac{1}{\sqrt{L_L C_L}} \\ \omega_{se} = \frac{1}{\sqrt{L_R C_L}} & \omega_{sh} = \frac{1}{\sqrt{L_L C_R}}. \end{array} \tag{6}$$

The series resonant frequency ω_{se} and the shunt resonant frequency ω_{sh} can be designed with the same value, where $\omega_{se} = \omega_{sh}$, then the phase constant can be simplified as in Equation (7):

$$\beta(\omega) = \omega\sqrt{L_R C_R} - \frac{1}{\omega\sqrt{L_L C_L}}. \tag{7}$$

It is illustrated, in Equation (7), that this CRLH structure shows a "left-hand" property under low frequencies, and it shows a "right-hand" property under high frequencies. The resonant frequency is obtained when the phase value is zero, where $\beta(\omega) = 0$.

$$\omega_0 = \sqrt{\omega_L\omega_R} = \frac{1}{\sqrt[4]{L_R C_R L_L C_L}}. \tag{8}$$

If the SIW TL section (as shown in Figure 1a) is taken into account, then the total phase shift of the CRLH filter on achieving a zeroth order mode can be written as [25]:

$$\beta l = 2\phi_C + \phi_{SIW} = 0 \tag{9}$$

where ϕ_C is the phase shift due to two CRLH units, and ϕ_{SIW} is the phase shift due to the *SIW* section:

$$\phi_C = \omega\sqrt{L_R C_R} - \frac{1}{\omega\sqrt{L_L C_L}} \tag{10}$$

$$\phi_{SIW} = \frac{2\pi}{\lambda_g} = \frac{2\pi}{\lambda_0}\sqrt{1 - \left(\frac{\lambda_0}{2a_{eff}}\right)^2} \tag{11}$$

where a_{eff} is the effective width of the SIW TL. Then, a resonate frequency can be derived by putting Equations (10) and (11) into Equation (9) and solving the equation:

$$\omega = \frac{\frac{\pi}{\lambda_0}\sqrt{1-\left(\frac{\lambda_0}{2a_{eff}}\right)^2} + \sqrt{\left(\frac{\pi}{\lambda_0}\right)^2\left[1-\left(\frac{\lambda_0}{2a_{eff}}\right)^2\right] + 4\frac{\sqrt{L_R C_R}}{\sqrt{L_L C_L}}}}{2\sqrt{L_R C_R}}. \quad (12)$$

We show in Equation (12) that the SIW TL section gives us more freedom to tune the operation frequency of the CRLH filter by optimizing the effective width of the SIW TL section (a_{eff}). Consequently, the CRLH filter with SIW TL section shows the potential to achieve a compact size.

The equivalent inductances and capacitances of the CRLH units are still dominant factors that determine the filter response. We illustrate, in Equation (8), that a resonation is generated by this CRLH structure, and the value of the resonant frequency is dominated by the capacitances and inductances introduced by the right-hand and left-hand effect. L_R and L_L are obtained solely by the metallic vias between the plates, which is fixed in the design. Consequently, C_R and C_L, provided by the interdigital capacitance and ground-coupling capacitance, become the only alterable elements, which results in a difficulty in achieving the desired value to resonate at the sub-6G frequency band. In this paper, the capacitances are enhanced by introducing the sawtooth interdigital-shaped CRLH unit, as shown in Figure 2a. The equivalent circuit of the proposed SIW filter is illustrated in Figure 2b.

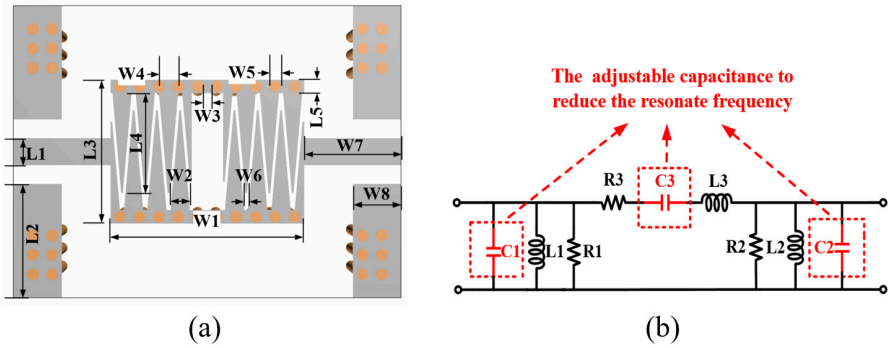

Figure 2. (**a**) Proposed SIW filter with interdigital sawtooth CRLH units and (**b**) the equivalent circuit of the proposed SIW filter.

In the equivalent circuit, R_1, R_2, and R_3 are the series and shunt resistances of the lossy material. C_1 and C_2 are generated by the right-handed capacitances (C_R) of the two CRLH units, while C_3 is generated by the left-handed capacitances (C_L) of the two CRLH units. Consequently, C_1 and C_2 are determined by the area of the sawtooth plates of the CRLH units, and C_3 is determined by the length of the interdigital slots of the CRLH units. Thus, the values of both C_1 and C_2 are increased by the proposed sawtooth CRLH units because of the larger plate area, compared with the conventional rectangular interdigital CRLH units. The value of C_3 is also increased because of the longer slots introduced by the sawtooth structure.

An AWR design environment software is used to simulate this filter. The equivalent circuit elements can be derived by generating a special model, which is achieved by simulating the frequency response of the filter using the AWR software. Capacitance values are simulated utilizing the proposed and conventional CRLH units with the same width W1 and length L3, as shown in Figure 3. The values of C_1 and C_2 are the same, since the two CRLH units in the filter are symmetrical. It is shown that, when the slot length L4 changes from 4.5 mm to 5.5 mm, the average value of C_1 and C_2 of the conventional rectangular CRLH units is 20 pF, while it is about 30 pF for the proposed sawtooth CRLH units. The average value of C_3 of the conventional rectangular CRLH units is 40 pF, while it is about 60 pF for the proposed sawtooth CRLH units. Consequently, the coupling capacitor of the filter is

increased by about 50% by the proposed sawtooth CRLH unit, the working frequency is possibly lower than 6 GHz, and a sub-6 GHz filter can be designed and implemented based on the proposed structure.

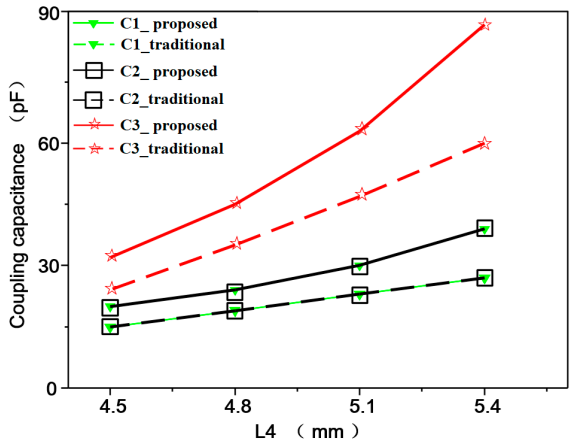

Figure 3. Simulated capacitance with different L4 slot lengths.

Generally, the sawtooth structure slots improve the flexibility of the design of the CRLH properties, as well as the miniaturization design, according to the theory discussed in this section.

Input matching is a key issue for the RF filter; it determines the reflection properties at the input and output terminals. In this work, the input and output impedance are well matched by optimizing the width of the input and output feeding line (L1). The input impedance characteristic, with different L1 lengths, is shown in Figure 4. It is illustrated that, when L1 is 1.4 mm, the input impedance of the filter is near the 50 ohm point on the smith chart. Consequently, the impedance can be well matched to 50 ohm by choosing a value of 1.4 mm for L1.

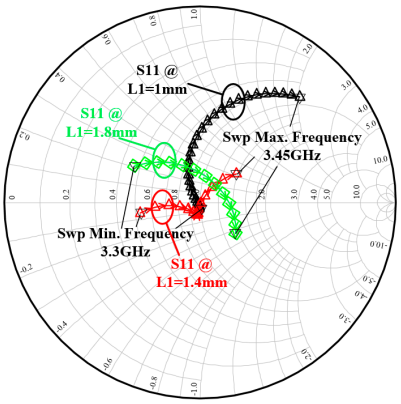

Figure 4. Impedance matching properties, with different L1 lengths.

The current distribution can be simulated by performing an EM simulation using the AXIEM simulator in the AWR software. The current distributions of the proposed filter, at frequencies of 2.5 GHz, 3.35 GHz, 3.4 GHz, and 4.0 GHz, are simulated and illustrated in Figure 5. The normalized current density is 1.5×10^5 A/m. This shows that, at the 3.35 GHz and 3.4 GHz passband frequencies, the current is well transferred from the input terminal to the output terminal. At the 2.5 GHz and 4.0 GHz stopband frequencies, the current is constrained at the input, so that the signal transfer through this filter is rejected at these frequencies. Therefore, the proposed filter shows the capacity of letting the passband signals go through the device and rejecting the stopband signals. Consequently, a compact CRLH filter for sub-6G systems with a low loss and high selectivity is well designed and optimized.

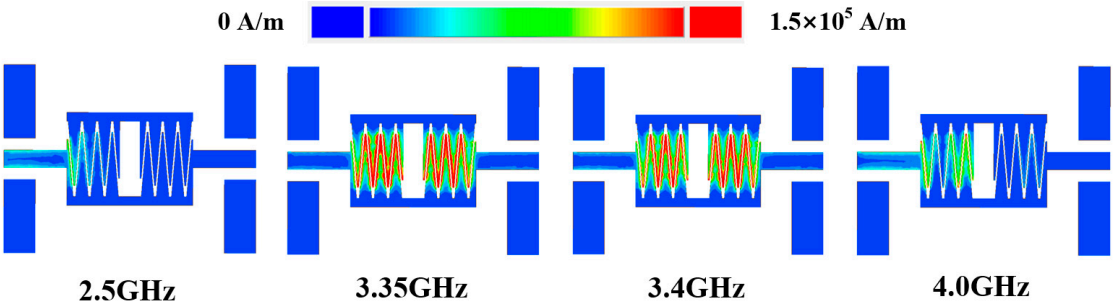

Figure 5. Current distribution of the proposed filter at different frequencies.

3. Filter Design and Measurement

To achieve a good matching and low insertion loss for the filter, the physical dimensions of every section in the proposed filter are carefully designed. The input matching is mainly determined by the width of the input feeding line (L1). The filter parameters are well optimized to achieve a good performance for the proposed filter. Finally, the physical dimensions of the proposed filter are designed as shown in Table 1: L1 = 1.4 mm, L2 = 5.8 mm, L3 = 7.4 mm, L4 = 5.1 mm, L5 = 0.7 mm, W1 = 10 mm, W2 = 1 mm, W3 = 0.5 mm, W4 = 1 mm, and W5 = 0.6 mm.

Table 1. Dimensions of the proposed filter.

Physical	Value (mm)	Physical Size	Value (mm)
W1	10	*L1*	1.4
W2	1	*L2*	5.8
W3	0.5	*L3*	7.4
W4	1	*L4*	5.1
W5	0.6	*L5*	0.7

To further demonstrate the merit of the proposed filter, a SIW filter, based on the proposed sawtooth interdigital CRLH units, was implemented with RT6010 material, the dielectric constant of which is 10.2, as shown in Figure 6. The core filter size is only 10 mm × 7.4 mm.

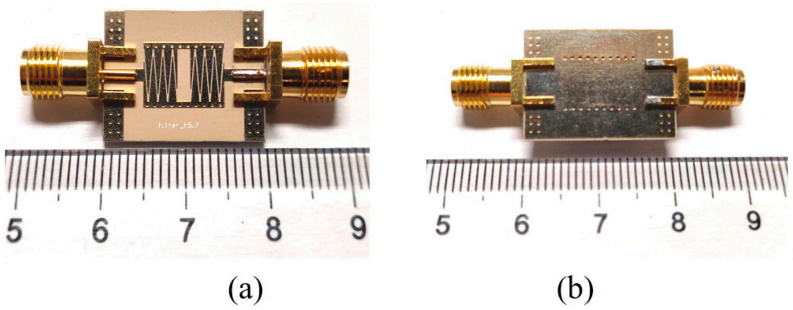

Figure 6. Photo of the proposed filter: (**a**) topside; and (**b**) backside.

The input and output signal are fed in and out through the RF SMA (Small A Type) connectors. The S parameter measurement results are shown in Figure 7. Figure 7 shows that the working frequency band of this proposed filter ranges from 3.25 GHz to 3.45 GHz, and the minimum insertion loss S21 is only 2.4 dB. The measured passband insertion loss is higher than the simulated result due to the additional loss introduced by the SMA connectors. The SMA connectors also introduce small parasitic inductances, which introduce additional serial inductances into the input and output. Consequently, the measured operation frequency band is about 100 MHz lower than the simulation result, as shown in Figure 7. The stopband rejection is better than −20 dB throughout the frequencies below 3.0 GHz

and above 3.8 GHz, and S11 is as low as −37 dB at 3.35 GHz. Hence, a novel compact CRLH SIW filter is successfully designed and implemented for a sub-6G application.

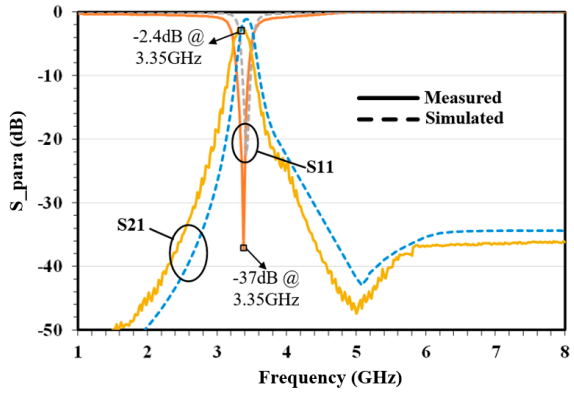

Figure 7. Measured S parameters of the proposed filter.

The phase response of S21 is measured for the proposed filter, as shown in Figure 8. Figure 8 shows that the phase response of S21 changes linearly throughout 3.25–3.45 GHz operation frequency band, indicating the small phase distortion of the proposed filter. A group delay is usually used to judge the nonlinear distortion of a filter. If the group delay ripple is large during the passband, then the signal transmission time throughout the device shows a nonlinear variation at different frequencies. The group delay variation throughout the passband is only 1.4 ns, which is extremely low for such a compact SIW filter.

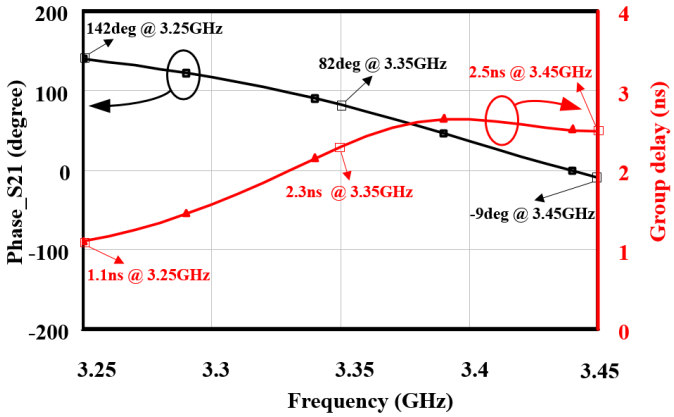

Figure 8. Measured phase and group delay of the proposed filter.

4. Discussion

Many studies have focused on improving the performance of the compact CRLH filter in recent years. The performance of several reported CRLH filters is summarized and compared in Table 2. The physical sizes of the reported filters are normalized by the wavelength of the center frequency (λ_0). The operation frequency of the filter, reported in [24], can be as low as 3 GHz, with a good bandwidth. However, the size of this filter is large ($0.8\ \lambda_0 \times 0.5\ \lambda_0$). In [25] and [26], two relatively compact filters using CRLH units are reported. However, their center operation frequencies are beyond the 6 GHz limitation. Two CRLH filters, presented in [27] and [28], are well designed for sub-6G applications. However, their sizes are still too large to meet the requirement of portable devices. For the design proposed in this work, the filter size is only $0.12\ \lambda_0 \times 0.09\ \lambda_0$, and the center frequency is only 3.35 GHz. We demonstrate that the proposed filter can be considered as one of the most compact CRLH filters with a low passband loss and high stopband rejection for sub-6G systems.

Table 2. Comparison of CRLH filters.

Ref.	Center Frequency (GHz)	Insertion Loss (dB)	Bandwidth (MHz)	Size ($\lambda_0 \times \lambda_0$)
[24]	3/6/9	3	150/500/300	0.8×0.5
[25]	6.8	3	200	0.23×0.14
[26]	7.3	2.2	50	0.40×0.32
[27]	5.3	2.7	500	0.51×0.13
[28]	5	2.7	700	0.37×0.25
This work	3.35	2.4	200	0.12×0.09

5. Conclusions

A novel SIW filter with modified sawtooth interdigital CRLH resonator units is proposed for sub-6G communication systems. The structures of both traditional rectangular and modified filters are discussed and compared. The proposed structure increases the coupling capacitance of the interdigital capacitor in CRLH units, reduces the filter resonant frequency and miniaturizes the filter size. The proposed filter is finally fabricated and tested, and a 3.25–3.45 GHz compact filter, with only a 2.4 dB insertion loss, is successfully realized for sub-6G portable devices.

Author Contributions: Conceptualization, S.H. and Y.H.; Data curation, S.H. and Y.H.; Formal analysis, H.Z.; Investigation, W.Z. and Y.G.; Methodology, S.H.; Writing—original draft, S.H.; Writing—review and editing, X.Z. All authors have read and agreed to the published version of the manuscript.

Funding: This work was financially supported by the National Natural Science Foundation of China (61501261) and the China Postdoctoral Science Foundation (2017M621793).

Conflicts of Interest: The authors declare no conflict of interest.

References

1. Huang, L.; Yuan, N. A Compact Wideband SIW Bandpass Filter with Wide Stopband and High Selectivity. *Electronics* **2019**, *8*, 440. [CrossRef]
2. Jia, D.; Feng, Q.; Xiang, Q.; Wu, K. Multilayer Substrate Integrated Waveguide (SIW) Filters with Higher-Order Mode Suppression. *IEEE Microw. Wirel. Compon. Lett.* **2016**, *26*, 678–680. [CrossRef]
3. Li, P.; Chu, H.; Zhao, D.; Chen, R.S. Compact Dual-Band Balanced SIW Bandpass Filter With Improved Common-Mode Suppression. *IEEE Microw. Wirel. Compon. Lett.* **2017**, *27*, 347–349. [CrossRef]
4. Lovato, R.; Gong, X. A Third-Order SIW Integrated Filter/Antenna Using Two Resonant Cavities. *IEEE Antennas Wirel. Propag. Lett.* **2018**, *17*, 505–508. [CrossRef]
5. Zhang, H.; Kang, W.; Wu, W. Miniaturized Dual-Band SIW Filters Using E-Shaped Slotlines with Controllable Center Frequencies. *IEEE Microw. Wirel. Compon. Lett.* **2018**, *28*, 3111–3313. [CrossRef]
6. Saghati, A.P.; Entesari, K. Ultra-Miniature SIW Cavity Resonators and Filters. *IEEE Trans. Microw. Theory Tech.* **2015**, *63*, 4329–4340. [CrossRef]
7. Sun, L.; Sun, B.; Yuan, J.P.; Tang, W.; Wu, H. Low Profile, Quasi-Omnidirectional, Substrate Integrated Waveguide (SIW) Multi-Horn Antenna. *IEEE Antennas Wirel. Propag. Lett.* **2015**, *15*, 818–821. [CrossRef]
8. Martinezros, A.J.; Gomeztornero, J.L.; Goussetis, G. Multifunctional Angular Bandpass Filter SIW Leaky-Wave Antenna. *IEEE Antennas Wirel. Propag. Lett.* **2017**, *16*, 936–939. [CrossRef]
9. Jin, H.; Luo, G.Q.; Wang, W.; Che, W.; Chin, K.S. Integration Design of Millimeter-Wave Filtering Patch Antenna Array with SIW Four-Way Anti-Phase Filtering Power Divider. *IEEE Access* **2019**, *7*, 49804–49808. [CrossRef]
10. Hesari, S.S.; Bornemann, J. Design of a SIW Variable Phase Shifter for Beam Steering Antenna Systems. *Electronics* **2019**, *8*, 1013. [CrossRef]
11. Ebrahimpouri, M.; Nikmehr, S.; Pourziad, A. Broadband Compact SIW Phase Shifter Using Omega Particles. *IEEE Microw. Wirel. Compon. Lett.* **2014**, *24*, 748–750. [CrossRef]
12. Ghaffar, F.A.; Shamim, A. A Partially Magnetized Ferrite LTCC Based SIW Phase Shifter for Phased Array Applications. *IEEE Trans. Magn.* **2015**, *51*, 1–8. [CrossRef]

13. Muneer, B.; Qi, Z.; Shanjia, X. A Broadband Tunable Multilayer Substrate Integrated Waveguide Phase Shifter. *IEEE Microw. Wirel. Compon. Lett.* **2015**, *25*, 220–222. [CrossRef]
14. Nafe, A.; Shamim, A. An Integrable SIW Phase Shifter in a Partially Magnetized Ferrite LTCC Package. *IEEE Trans. Microw. Theory Tech.* **2015**, *63*, 2264–2274. [CrossRef]
15. Djerafi, T.; Hammou, D.; Wu, K.; Tatu, S.O. Ring-Shaped Substrate Integrated Waveguide Wilkinson Power Dividers/Combiners. *IEEE Trans. Compon. Packag. Manuf. Technol.* **2014**, *4*, 1461–1469. [CrossRef]
16. Khan, A.A.; Mandal, M.K. Miniaturized Substrate Integrated Waveguide (SIW) Power Dividers. *IEEE Microw. Wirel. Compon. Lett.* **2016**, *26*, 1–3. [CrossRef]
17. Danaeian, M.; Moznebi, A.R.; Afrooz, K.; Hakimi, H. Miniaturised equal/unequal SIW power divider with bandpass response loaded by CSRRs. *Electron. Lett.* **2016**, *52*, 1864–1866. [CrossRef]
18. Huang, Y.M.; Jiang, W.; Jin, H.; Zhou, Y.; Leng, S.; Wang, G.; Wu, K. Substrate-Integrated Waveguide Power Combiner/Divider Incorporating Absorbing Material. *IEEE Microw. Wirel. Compon. Lett.* **2017**, *27*, 1–3. [CrossRef]
19. Jin, H.; Zhou, Y.; Huang, Y.M.; Ding, S.; Wu, K. Miniaturized Broadband Coupler Made of Slow-Wave Half-Mode Substrate Integrated Waveguide. *IEEE Microw. Wirel. Compon. Lett.* **2017**, *27*, 132–134. [CrossRef]
20. Liu, Z.; Xiao, G. Design of SIW-Based Multi-Aperture Couplers Using Ray Tracing Method. *IEEE Trans. Compon. Packag. Manuf. Technol.* **2017**, *7*, 106–113. [CrossRef]
21. Lian, J.W.; Ban, Y.L.; Zhu, J.Q.; Kang, K.; Nie, Z. Compact 2-D Scanning Multibeam Array Utilizing SIW Three-Way Couplers at 28 GHz. *IEEE Antennas Wirel. Propag. Lett.* **2018**, *17*, 1915–1919. [CrossRef]
22. Hagag, M.F.; Zhang, R.; Peroulis, D. High-Performance Tunable Narrowband SIW Cavity-Based Quadrature Hybrid Coupler. *IEEE Microw. Wirel. Compon. Lett.* **2018**, *29*, 1–3. [CrossRef]
23. Lee, J.G.; Lee, J.H. Zeroth Order Resonance Loop Antenna. *IEEE Trans. Antennas Propag.* **2007**, *55*, 994–997. [CrossRef]
24. Mohan, M.P.; Alphones, A.; Karim, M.F. Triple Band Filter Based on Double Periodic CRLH Resonator. *IEEE Microw. Wirel. Compon. Lett.* **2018**, *28*, 212–214. [CrossRef]
25. Abdalla, M.A.; Mahmoud, K.S. A compact SIW metamaterial coupled gap zeroth order bandpass filter with two transmission zeros. In Proceedings of the International Congress on Advanced Electromagnetic Materials in Microwaves & Optics, Chania, Greece, 19–22 September 2016.
26. Daw, A.F.; Hussein, O.T.; Abdelhamid, H.S.; Abdalla, M.A. Ultra compact quad band resonator based on novel D-CRLH configuration. In Proceedings of the 2017 IEEE International Symposium on Antennas and Propagation & USNC/URSI National Radio Science Meeting, San Diego, CA, USA, 9–14 July 2017.
27. Yang, T.; Chi, P.L.; Xu, R.; Lin, W. Folded Substrate Integrated Waveguide Based Composite Right/Left-Handed Transmission Line and Its Application to Partial -Plane Filters. *IEEE Trans. Microw. Theory Tech.* **2013**, *61*, 789–799. [CrossRef]
28. Karim, M.F.; Ong, L.C.; Luo, B.; Chiam, T.M. A compact SIW bandpass filter based on modified CRLH. In Proceedings of the 2012 Asia Pacific Microwave Conference Proceedings, Kaohsiung, Taiwan, 4–7 December 2012.